Influence of doping with silver nanoparticles on the molybdenum trioxide gas sensor prepared by spray pyrolysis

A. H. A. Alrazak [a], S. H. Salman [a], I. A. Abbas [b], M. H. Mustafa [a], H. M. Ali [a*], S. A. Abbas [a]
[a] *Department of Physics, College of Education for Pure Science (Ibn-Alhaitham), University of Baghdad –Iraq,*
[b] *Department of Physics, College of Education, Mustansiriyah University*

By spray pyrolysis method, Molybdenum trioxide films are deposited at 400 °C and doped with silver nanoparticles at different concentrations between (1 and 3) mM. X-ray diffraction (XRD), Atomic force microscopy (AFM), Field-emission scanning electron microscopy (FE-SEM), UV-vis spectroscopy, used to examine the physical properties films. According to XRD data, doping enhances the crystalline quality of deposited MoO_3 thin films, which crystallize in an orthorhombic structure with a (021). The enargy gap was found (2.85 - 2.59) eV in films. The performance of gas sensing in the movie CO_2 Different ratios of silver nanoparticles (0, 1, and 3 mM) were used for gas measurements. It was discovered that the gas detecting system's performance had greatly increased.

(Received November 23, 2024; Accepted February 21, 2025)

Keywords: UV, Molybdenum trioxide, Spray pyrolysis, Gas sensor

1. Introduction

MoO_3 is an n-type semiconductor that exist in four phases: orthorhombic (α-MoO3), monoclinic (β-MoO_3), hexagonal (h-MoO_3), and ε-MoO_3. It possesses intriguing physical properties [1-4]. The growth conditions and the chosen thin film deposition process have a significant impact on the phase, morphology of films [5]. Numerous metal oxides can be used for gases sensing such as V_2O_3, Fe_2O_3, Cr_2O_3, Co_3O_4, NiO, SrO, In_2O_3, TiO_2, MoO_3, Nd_2O_3, CuO, WO_3, GeO_2, Nb_2O_5 by measurement the variation their resistance due to the gas adsorption on the surface reign of the films [6,7].

Numerous physical and chemical techniques, including nebulizer spray pyrolysis [1], electron beam evaporation [8], Radio Frequency magnetron sputtering [9], Thermal Evaporation [10], laser-assisted evaporation [11], etc., It is used to prepare thin films of MoO_3.

In this work, simple spray pyrolysis was used to prepare MoO_3:Ag films.

AFM, (XRD), (FE-SEM), and UV-VIS have all been employed to analyze the generated films' physical properties in relation to their Ag concentration, and design gas sensor to detected gas (CO_2).

2. Experimental

From a solution of ammonium molybdatetetrahydrate [$(NH_4)_6Mo_7O_{24}$], Molybdenum trioxide thin films deposited on glass. After dissolving a part of it in distilled water, the mixture is agitated with a magnetic stirrer for thirty minutes at R.T until it becomes translucent and clear. at a concentration of 0.03 M molar.The following relationship indicates how much [$Ni(NO_3)_2{,}_6H_2O$] is required to create the solution: [12].

* Corresponding author: hiba.m.a@ihcoedu.uobaghdad.edu.iq
https://doi.org/10.15251/DJNB.2025.201.191

$$W_t = M.Mwt.V \tag{1}$$

Examine the physical properties of MoO3 films after deposition. Molybdenum trioxide films were produced by spraying the pre-made pyrolysis solution onto the glass at 400 °C, placing it on a rotating base, and using a spray rate of 0.25 mL/s. The films were deposited with varying ratios of silver nanoparticles (0, 1, and 3 mmol). Cu Kα radiation is used in an x-ray diffractometer (XRD) to verify the structural characteristics. To analyze the properties of the sample placed on glass, the SHIMADZU UV-VIS spectrophotometer was used. Surface morphologies are examined using the FESEM. (AFM) was used to analyze the surface topography. The Crystallite size (D) can be ascertained using by Scherrer's eq. [13,14].

$$\mathbf{D} = \frac{0.94\lambda}{\beta \cos\theta} \tag{2}$$

β the width at half maximum intensity. The following formula may be used to get the micro strain for the generated sample. [15-18] :

$$\varepsilon = \frac{\beta hkl}{4\tan\theta} \tag{3}$$

The number of crystallites per area and the density of dislocation, which can be calculated using the relationships below [19-23].

$$\delta = \frac{1}{Cs^2} \tag{4}$$

$$N_0 = \frac{1}{Cs^2} \tag{5}$$

t: thickness of thin film with (200∓25 nm)

The UV-visible 1800 spectrophotometer measures transmittance and absorbance at wavelengths between 200 and 1200.
(AL) was evaporated as ohmic contact electrodes in of the MoO_3 and MoO_3:Ag gas sensors. The rate of change in resistance of films upon exposure to gas is a popular way to determine a film's gas sensitivity. By calculating the responses, the sensitivity of the sensors may be evaluated [24,25].

$$S\% = ((R_g - R_a)/ R_a) \times 100\% \tag{6}$$

Ra and R_g: film resistance in air and in the presence of gas respectively.

3. Results

3.1. Microstructures and morphology

Fig. 1 displays the XRD pattern for different Ag-doped MoO_3 film concentrations. According to Fig. 1, showed thin films have a polycrystalline structure that includes orientations along different planes, are (040), (021), (111) and (060). Peak (021) is the strongest.
MoO_3 monoclinic structure is confirmed by all of the diffraction peaks (JCPDS No. 47–1320 card). The strength of the planes increases with increasing doping concentration, suggesting that the substitution of Ag doping elements is leading to a rising crystalline 3% Ag doping concentration.

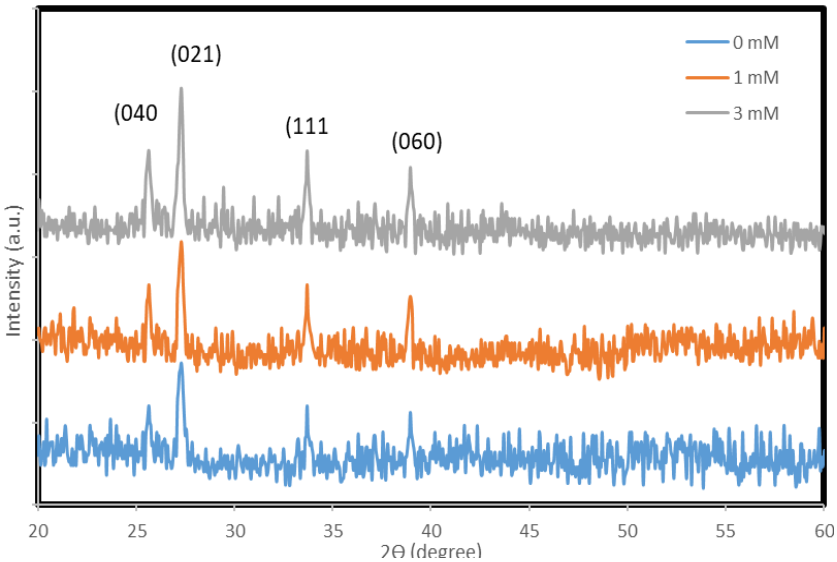

Fig. 1. XRD pattern of MoO_3 and MoO_3: Ag films.

Figure 1 represents an X-ray diffraction diagram from which it is clear that the intensity of the peak increases while the width of the peak decreases, and there is a slight deviation of the peak from its position with the increase in the percentage of doping. These results agree well with [26-28], this is due to the irregular stress on the crystalline structure of the films arising from crystalline defects. The parameters of the prepared films were calculated. We note that the grain size decreases, while the dislocations, microductility, and the number of crystals increase with the increase in the doping ratio. This is as a result of increasing grain boundaries as a result of the substitution of Ag ions with MoO3 ions and also due to surface tension, the volume area ratio increases, meaning the surface roughness of the films increases, and this is consistent with the AFM results.

Table 1. Variation of structural parameters in Ag-doped MoO_3 thin films.

Ag Con. (mM)	2θ(deg.) Exp.	D (nm)	δ*1014 (lines/m2)	ε	N0x10^{15} (m-2)
0	25.68	69.752	2.055	0.519	0.589
	27.28	49.353	4.106	0.733	1.664
	33.68	57.420	3.033	0.630	1.056
	38.92	61.558	2.639	0.588	0.857
1	25.66	64.465	2.406	0.561	0.747
	27.25	46.653	4.595	0.776	1.970
	33.65	52.864	3.578	0.685	1.354
	38.88	56.062	3.182	0.646	1.135
3	25.63	57.493	3.025	0.630	1.052
	27.21	44.232	5.111	0.818	2.311
	33.61	48.976	4.169	0.739	1.702
	38.82	52.695	3.601	0.687	1.367

3.2. Morphological analysis of MoO3:Ag thin films

Figure 2 shows images of the AFM results. Through analyzing the measurements, we note that the doping process clearly affected the surface parameters of the prepared MoO_3 films, as it was found that the surface grains are more homogeneous, with a decrease in their roughness values, based on the values of the square root of the mean square of roughness, compared to the surface of the undoped films. The roughness depends on distribution of molecules spread on the surfaces of the films, as well as the appearance of the nanostructures of the prepared films [20]. The variation in the properties of the membrane leads to a variation in the optical properties, and this is consistent with the results of the visual examination.

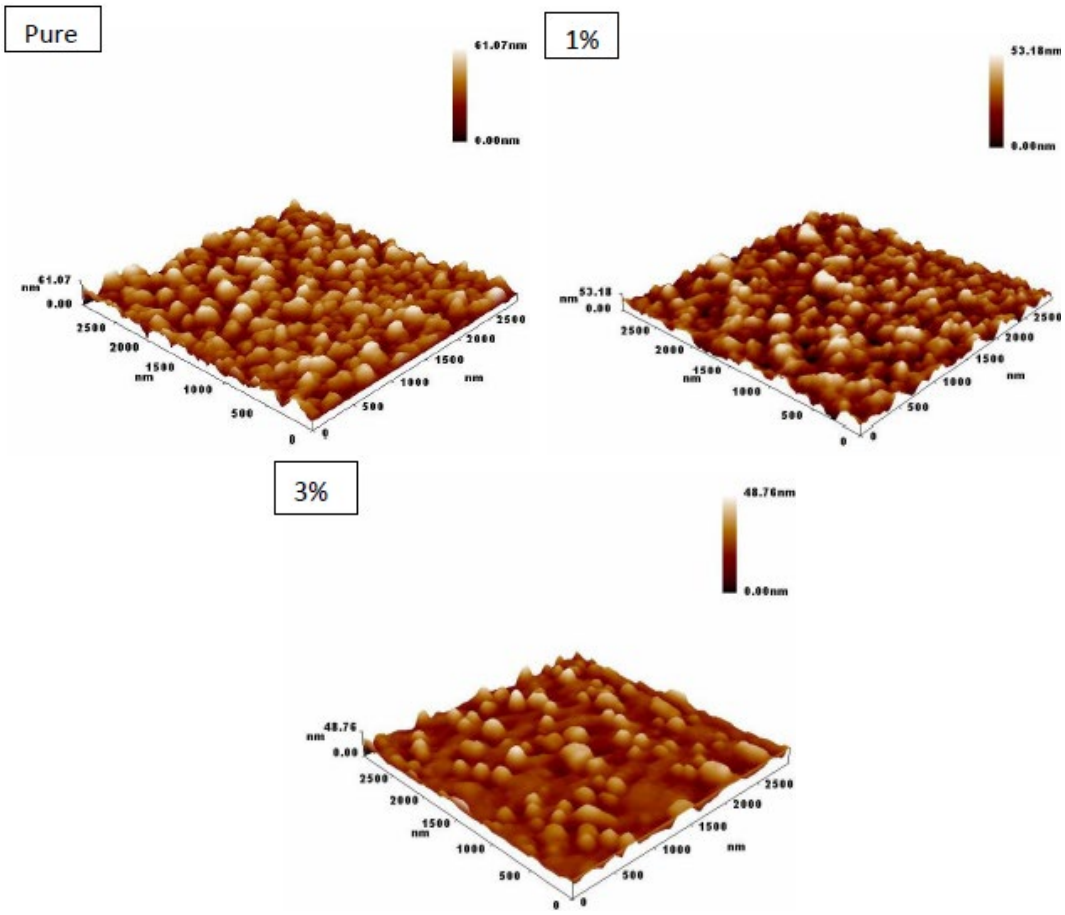

Fig. 2. Shows images of the AFM results, for MoO_3 and MoO_3:Ag.

3.3. FE-SEM

Fig. 3 shows FESEM micrographs of Ag-doped and undoped MoO_3 thin films. A surface that is clearly disturbed, with a rough shape and a randomly aligned chain-like structure (of varied diameters), is observed in an undoped MoO_3 film that was investigated using a FESEM. On the other hand, the formation of massive chain-like structures along with numerous holes suggests that doping with 3% Ag is crucial for crystallinity.

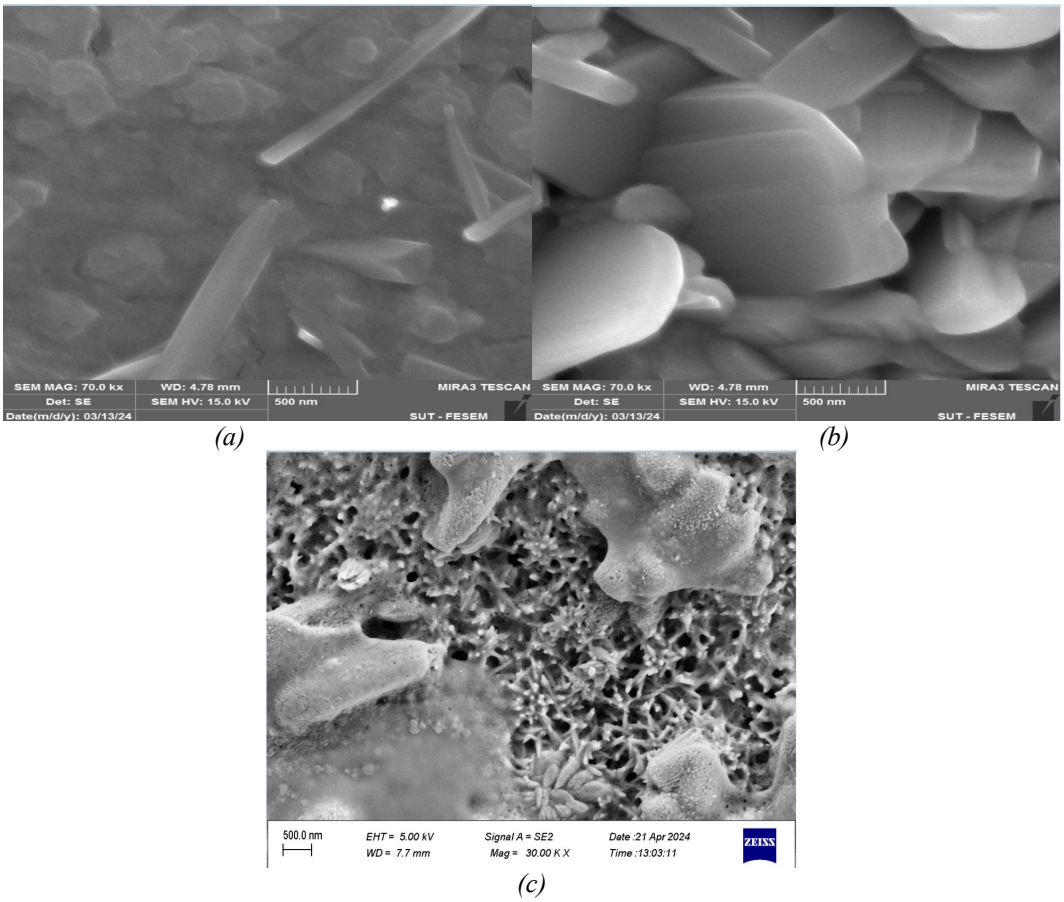

Fig. 3. (FE-SEM)MoO_3 films with different con. Ag (a) 0%, (b) 1%, (c) 3% and (d) cross section of MoO_3 film.

3.4. Optical properties

Fig 4 represents the spectrum of transmittance and absorbance of the prepared films. We note that the transmittance of all films increases with increasing $\boldsymbol{\lambda}$ nm, since the visible and near-infrared regions had the highest transmittance, which was measured at almost 70%, which indicates that these films are not suitable for being solar cells, but are useful in Apply smart windows and coatings to various surfaces [23],and note the presence of peaks in the visible region indicating homogeneity Prepared films, where doping had an effect on the permeability values. We notice from the absorption and transmittance spectra in Figure (4) the appearance of surface plasmon resonance (SPR) peaks for the MoO3:Ag films at the wavelengths (LSPR = 559, 567) nm as a function of changing the silver doping ratios (1, 3) mM, respectively, as a result of the presence of silver nanoparticles [29,30], as shown in Table (2). The existence of these peaks denotes the emergence of nanoparticles in the doped films, and raising the doping ratios causes more nanoparticles to develop, which raises the MoO_3:Ag films' absorbance values. The appearance of the SPR peak with increasing doping ratios was towards the long wavelength (red shift) as a result of Mie scattering. The results of the effect of increasing the doping ratios of tungsten dioxide films with gold nanoparticles were in agreement with the results of studies [31]. As the percentage of doping increases, the permeability decreases due to the formation of levels of impurity Ag inside the energy gap. These levels are prepared to receive electrons and generate tail levels that work to reduce the value of the energy gap. As for the absorbance curve, it is opposite in its behavior to the permeability curve. We notice the absorbance increases, and this indicates that photons with low energies, less than the energy of the net energy gap, are absorbed to a greater extent after doping, meaning that it does not enable it to excite the electrons and relocate them from the valence to conduction band.

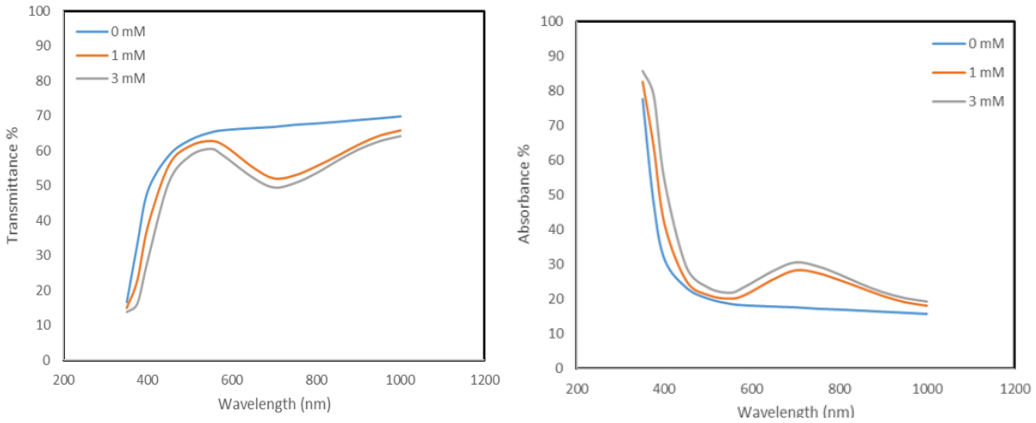

Fig. 4. Spectral transmittance and Absorbance curves for MoO_3 and MoO_3: Ag films.

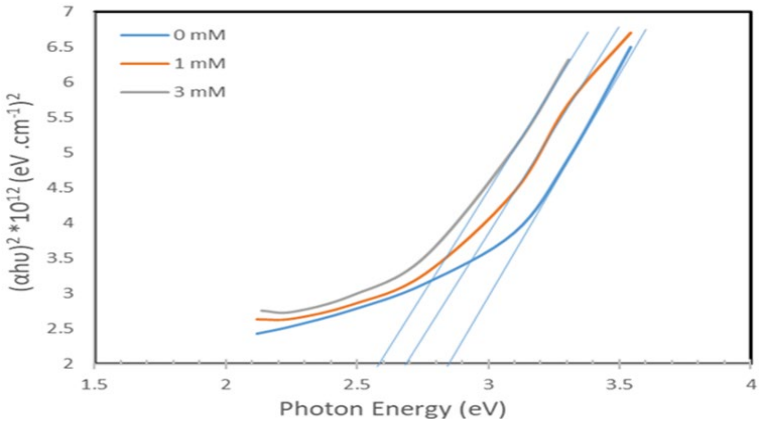

Fig. 5. Plot of $(\alpha h\nu)^2$ with $(h\nu)$ for MoO_3 films at different concentration of Ag NPs.

Fig 5 shows the value of (Eg opt.) for the films. We notice that the energy gap values decrease with the increase in the doping ratio due to the local levels (donor level) that are generated due to the doping material that is located below the conduction band and is prepared to receive electrons and the transitions are of the direct type allowed, in general, the results of optical measurements are consistent with the results of the research group [10,28,31-37].

Table 2. Optical parameters variation of Ag Concentration doped MoO_3 thin films.

Ag Concentration (mM)	Eg (eV)	FWHM (nm)	λ SPR (nm)
0	2.85	……	……
1	2.7	200	559
3	2.59	218	567

3.5. Gas senor tests

By examining films, they gave an n-type, as a result of their resistance increasing when exposed to CO_2, which is normal for n-type semiconductors that react with oxidizing gas [38]. The sensitivity of the sensors can be calculated using Equation (6) and the change in sensitivity with time is shown in (Fig. 6).

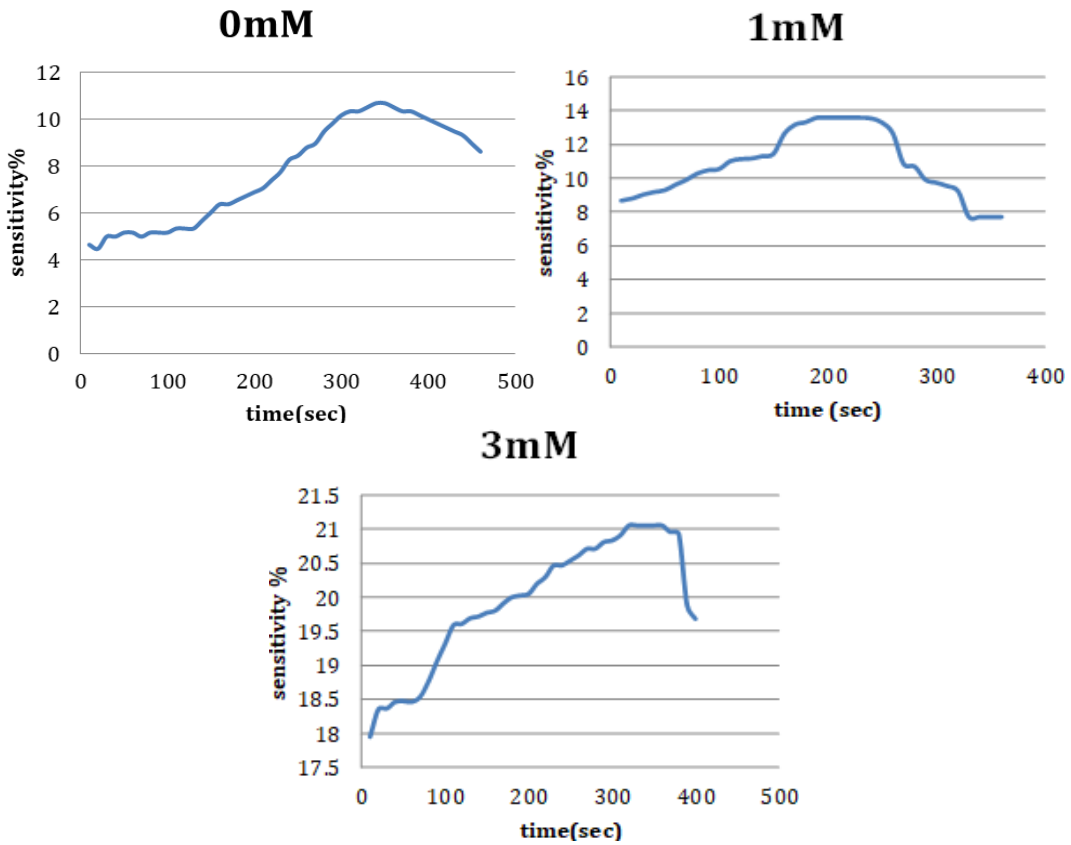

Fig. 6. Shows of variation of Ag Concentration doped MoO_3 thin films on Gas sensitivity for gas CO_2.

Table 3. Sensitivity changes with Ag Concentration (mM).

Ag Concentration (mM)	sensitivity
0	10.68
1	13.58
3	21.05

We notice from the fig. (6) and table 3, that sensitivity increases with increasing silver concentration due to a decrease in Crystallite size (D) and increase in the number of crystals per unit area. So, it will increase the surface area relative to the volume, that is, an increase in the surface roughness. Thus, increasing the adsorption of gas molecules. [39,40]

4. Conclusions

Molybdenum trioxide thin films are deposited at 400 °C and doped with silver nanoparticles at different concentrations between (1 and 3) mM. Through structural testing of the produced films, we determined that the films have nanostructures and that doping had an impact on the structure. We observe that as the percentage of doping increases, there is a corresponding drop in Crystallite size (D) and increase in the number of crystals per unit area. So it will increase the surface area relative to the volume, that is, an increase in the surface roughness. Therefore, these films can be used as a gas sensing application, and we conclude from optical examinations that the doping led to a decrease in transmittance and an increase in absorbance. Highest transmittance (70%). Additionally, we observe that the energy gap shrinks as the doping ratio

rises, a sign that the doped films' conductivity is rising, which was recorded from (2.85-2.59 eV) due to the generation of local levels within the optical energy gap due to doping material these levels are prepared to receive electrons, so resistance decreases. Sensitivity is maximum for MoO3: Ag thin films at (3mM) among all thin films. is 21.05 %,

References

[1] F. H. Alkallas, A. Ben Gouider Trabelsi, M. Shkir, S. AlFaify, Nanomaterials, vol. 12, no. 16, p. 2797, 2022; https://doi.org/10.3390/nano12162797

[2] S. Boyadzhiev, V. Lazarova, M. Rassovska, I. Yordanova, R. Yordanov, Optoelectronics and Advanced Materials-Rapid Communications, vol. 4, no. 10, pp. 1485-1488, 2010.

[3] C. Castillo et al., Journal of the Chilean Chemical Society, vol. 61, no. 1, pp. 2816-2820, 2016; https://doi.org/10.4067/S0717-97072016000100014

[4] S. Yang et al., Sensors and Actuators B: Chemical, vol. 226, pp. 478-485, 2016; https://doi.org/10.1016/j.snb.2015.12.005

[5] S. Subbarayudu, V. Madhavi, S. Uthanna, Adv. Mater. Lett, vol. 4, no. 8, pp. 637-642, 2013; https://doi.org/10.5185/amlett.2012.11466

[6] H.M. Ali, E. Kh. Shokr, Y.A. Taya, Sh. A. Elkot, M.F. Hasaneen, W.S. Mohamed, J. Sensors and Actuators A Physical 335(1):113355, 2022; https://doi.org/10.1016/j.sna.2021.113355

[7] Seham H. Salman 1, Sarab S. Jahil, N. A. Hassan, Shaimaa A. Abbas, Kareem A. Jasim, Journal of Physics: Conference Series 2857 (2024) 012051; https://doi.org/10.1088/1742-6596/2857/1/012051

[8] R. Sivakumar, R. Gopalakrishnan, M. Jayachandran, C. Sanjeeviraja, Current Applied Physics, vol. 7, no. 1, pp. 51-59, 2007; https://doi.org/10.1016/j.cap.2005.10.001

[9] S. Subbarayudu, V. Madhavi, S. Uthanna, ISRN Condensed Matter Physics, vol. 2013, pp. 1-9, Sep. 2013; https://doi.org/10.1155/2013/806374

[10] H. M. M. Arachchige, E. Comini, D. Zappa, G. Sberveglieri, Proceedings, MDPI, 2017, p. 449. Accessed: Jul. 28, 2024; https://doi.org/10.3390/proceedings1040449

[11] Y. A. Pastrana, J. Torres, L. D. López-Carreño, H. M. Martínez, J Supercond Nov Magn, vol. 26, no. 7, pp. 2475-2478, Jul. 2013; https://doi.org/10.1007/s10948-012-1721-z

[12] M. H. Mustafa, A. A. Shihab, Journal of Ovonic Research, vol. 19, no. 6, 2023; https://doi.org/10.15251/JOR.2023.196.623

[13] A. Z. Obaid, M. H. Mustafa, H. K. Hassun, AIP Conference Proceedings, AIP Publishing, 2020.

[14] M. Hamid, S. A. Fadaam, L. A. Mohammed, B. H. Hussein, Eurasian Chemico-Technological Journal, vol. 21, no. 2, pp. 183-185, 2019; https://doi.org/10.18321/ectj859

[15] H. M. Ali, M. H. Mustafa, Chalcogenide Letters, vol. 20, no. 6, pp. 431-437, 2023; https://doi.org/10.15251/CL.2023.206.431

[16] I. A. Abbas, S. Q. Hazaa, S. H. Salman, Journal of Physics: Conference Series, IOP Publishing, 2021, p. 032061; https://doi.org/10.1088/1742-6596/1879/3/032061

[17] Ali, H.M., Khudayer, I.H.Study structure and optical properties of Ag2Se, Ag2Se0.8Te0.2 an Ag2Se0.8S0.2 thin films, Journal of Ovonic Research, 2022, 18(5), pp. 675–680

[18] S. H. Salman, N. A. Hassan, G. S. Ahmed, Chalcogenide Letters, vol. 19, no. 2, pp. 125-130, 2022; https://doi.org/10.15251/CL.2022.192.125

[19] A. A. Shehab, S. H. Salman, Ibn AL-Haitham Journal For Pure and Applied Science, vol. 25, no. 1, 2017.

[20] S. H. Salman, E. A. Abbas, S. A. Abbas, Iraqi Journal of Science, pp. 1968-1974, 2016.

[21] S. H. Salman, S. M. Ali, G. S. Ahmed, Journal of Physics: Conference Series, IOP Publishing, 2021, p. 032058; https://doi.org/10.1088/1742-6596/1879/3/032058

[22] I. A. Abbas, S. Q. Hazaa, AIP Conference Proceedings, AIP Publishing, 2020;

https://doi.org/10.1063/5.0033226

[23] H. I. M. Mohammed, G. Sarhan Ahmed, S. Hassan Salman, I. Akram Abbas, S. M. Obaid, International Journal of Nanoelectronics and Materials, vol. 16, p. [749-758], 2023; https://doi.org/10.58915/ijneam.v16i3.1341

[24] Salman, S.H., Hassan, N.A., Ahmed, G.S., Mohammed, H.I., Abbas, S.A, 2024. Iraqi Journal of Applied Physics, V. 20, Issue 1, P. 37 - 42.

[25] Shatha Shammon Batros Jamil, Areej Adnan Hateef, Habiba Kadhim Atty, Physical Sciences Research International ,Vol. 3(2), pp. 18-25 ,(2015).

[26] B. H. Hussein, I. H. Khudayer, M. H. Mustafa, and A. H. Shaban,, *PIE*, vol. 13, no. 2, p. 173, 2019, https://doi.org/10.1504/PIE.2019.099358 .

[27] G. E. Buono-Core et al., Journal of non-crystalline solids, vol. 387, pp. 21-27, 2014; https://doi.org/10.1016/j.jnoncrysol.2013.12.009

[28] B. Ghasemi, F. Hajakbari, A. Hojabri, Inorganic and Nano-Metal Chemistry, vol. 50, no. 5, pp. 414-422, May 2020; https://doi.org/10.1080/24701556.2020.1716008

[29] C. Louis and O. Pluchery, Gold Nanoparticles For Physics, Chemistry And Biology (Second Edition). World Scientific, 2017; https://doi.org/10.1142/q0036

[30] Ali, H.M., Khudayer, I., Chalcogenide Letters, 2023, 20(3), pp. 197-203; https://doi.org/10.15251/CL.2023.203.197

[31] G. Morales-Luna, M. Morales-Luna, Scientific Reports, vol. 10, no. 1, p. 5841, 2020; https://doi.org/10.1038/s41598-020-62706-4

[32] Mustafa, M.H., Ali, H.M., Ahmed, G.S., Hussein, B.H., Chalcogenide Letters, 2023, 20(10), pp. 733-740; https://doi.org/10.15251/CL.2023.2010.733

[33] Mustafa, M.H., Ali, H.M., Habubi, N.F., Hussein, B.H., Journal of Materials Science: Materials in Electronics, 2024, 35(22), 1535; https://doi.org/10.1007/s10854-024-13259-z

[34] M. H. Mustafa, A. A. Shihab, Journal of Theoretical and Applied Physics, vol. 18(Special Issue), no.07, 2024, https://doi.org/10.57647/j.jtap.2024.si-AICIS23.07 .

[35] Salih, A.A., Ali, H.M., Athab, R.H., Hussein, B.H., Digest Journal of Nanomaterials and Biostructures, 2024, 19(2), pp. 981-988; https://doi.org/10.15251/DJNB.2024.192.981.

[36] Mustafa, M.H., Shehab, A.A., Fadaam, S.A., Abd, A.N.,IOP Conf. Series: Journal of Physics: Conf. Series 1003,(2018) 012121, https://iopscience.iop.org/article/10.1088/1742-6596/1003/1/012121#:~:text=DOI%2010.1088/1742%2D6596/1003/1/012121 .

[37] Mustafa, M.H., Hassun, H.K., Athab, R.H., ...Al-Maiyaly, B.K.H., Hussein, B.H., Journal of Ovonic Research 18(4), pp. 601-608 ,2022 ,https://doi.org/10.15251/JOR.2022.184.601 .

[38] Teodóra Nagyné-Kovács, Levente Studnicka, István Endre Lukács, Krisztina László, Pawel Pasierb, Imre Miklós Szilágyi, György Pokol,J. Nanomaterials 2020, 10, 891; https://doi.org/10.3390/nano10050891

[39] Fadaam, S.A., Ali, H.M., Shaban, A.H., Ahmed, S.A. Improving efficiency of solar cell for MnS through annealing,AIP Conference Proceedings, 2020, 2307, 020030**.** https://doi.org/10.1063/5.0033260

[40] Ali,H.M.,Hassun, H.K., Al-Maiyaly, B.K.H., Shaban, A.H., Fabrication and characterization of n-InSb Heterojunction for optoelectronic device, Energy Procedia, 2019, 157, pp. 90–99. https://doi.org/10.1016/j.egypro.2018.11.168